The temperature dependence of the magnetization distribution in $Fe_{65}Ni_{35}$ invar: incompatibility of the two-state model

2001 J. Phys.: Condens. Matter 13 1563

(http://iopscience.iop.org/0953-8984/13/7/317)

INSTITUTE OF PHYSICS PUBLISHING JOURNAL OF PHYSICS: CONDENSED MATTER

J. Phys.: Condens. Matter **13** (2001) 1563–1569 www.iop.org/Journals/cm PII: S0953-8984(01)19555-X

The temperature dependence of the magnetization distribution in $Fe_{65}Ni_{35}$ invar: incompatibility of the two-state model

P J Brown[1,2], **K-U Neumann**[2] **and K R A Ziebeck**[2]

[1] Department of Physics, Loughborough University, Loughborough LE11 3TU, UK
[2] Institut Laue Langevin, BP156 F 38042 Cedex, France

Received 29 November 2000

Abstract

The distribution of the magnetization in $Fe_{65}Ni_{35}$ invar has been studied as a function of temperature in the range 100 to 600 K using polarized neutron diffraction. The range in temperature covers the region over which the anomalous thermal expansion giving rise to the invar effect occurs. The polarized neutron results which have been analysed in terms of localized iron and nickel 3d moments with cubic anisotropy show that the fraction of unpaired electrons with e_g symmetry is approximately 47% and does not change with temperature. This is in contradiction to models of the invar effect which invoke the thermal population of two states with a different number of e_g and t_{2g} carriers.

1. Introduction

The invar effect was discovered more than 100 years ago by Guillaume [1]. He found that the face-centred cubic (fcc) alloys of iron and nickel containing roughly 35% of nickel ($Fe_{65}Ni_{35}$) have an almost zero thermal expansion coefficient over a broad temperature range. This useful property has been widely exploited in the construction of high precision mechanical instruments, but has as yet received no satisfactory microscopic explanation. In a recent volume of *Nature* [2, 3] it was claimed that the effect had been explained in microscopic detail. This claim was based on improved band structure calculations taking into consideration non-collinear components of the magnetization. However, neutron polarization analysis experiments [4] show that the only perpendicular components of the magnetization are those associated with spin waves. This contradiction serves to emphasise that although self-consistent band structure calculations give a reasonable account of the ground state properties of 3d metals and compounds the same is not true for the finite temperature properties of which the invar effect is one.

0953-8984/01/071563+07$30.00

1.1. The two-state model

The invar effect disappears above the Curie temperature, which suggests that the magnetic properties must in some way offset the normal lattice expansion and this premise is the foundation for most explanations given for the effect. Most theories are based on volume instabilities of the magnetic moments, which give rise to magneto-elastic coupling. The earliest model of this type was formulated by Weiss [5] who postulated that there are two possible states for fcc iron, the ferromagnetic high-volume state and the antiferromagnetic low-volume state. Thermally excited transitions between these states are supposed to compensate for the lattice expansion coming from anharmonic components of the lattice vibrations. Recent spin polarized band structure calculations made by Entel *et al* [6] lend support to this model. They predict the existence of at least two stable states in an fcc iron–nickel alloy which have different moments and atomic volumes. Although the thermodynamic consequences of this model are difficult to quantify, it has been suggested that the invar effect arises from the thermal population of the low-moment, low-volume state, which lies at a slightly higher energy than the high-moment state. To date there is no direct experimental evidence for the existence of these states. However, in Entel's calculations 3d-electrons in the two states are divided differently between the orbitals with e_g and t_{2g} symmetry. This means that the shape of the associated magnetization distributions differ. The magnetic moment of the higher energy state is supposed to be mostly due to electrons in t_{2g} orbitals, so the proportion of electrons with this symmetry in the mean distribution should rise with increasing temperature.

1.2. Finite temperature properties

Above the Curie temperature (T_c = 530 K) the uniform susceptibility has a strong temperature dependence indicating the presence of a substantial magnetic response in the paramagnetic phase. An estimate of the magnitude of this response can be made using a Curie–Weiss analysis [7]. This yields an effective paramagnetic moment p_{eff} of $\approx 3.3\ \mu_B$ and a paramagnetic moment μ_p of $\approx 2.45\ \mu_B$ per atom where $p_{eff}^2 = \mu_p(\mu_p+2)$. This value is larger than the average moment per atom $\langle\mu\rangle$ of $\approx 1.9\ \mu_B$ observed in the ground state. This casts serious doubts on models based on thermally induced high-spin to low-spin transitions. Band structure calculations cannot address the finite temperature properties which are usually discussed in terms of the thermal dependence of spin fluctuations [8]. However, models based on a single site spin fluctuation theory predict that the root mean square value of the *local moment* at T_c is reduced by a significant amount, typically 50%, from the ground state value [9]. A similar conclusion has been reported on the basis of thermal expansion and forced magnetostriction measurements [10]. Additional evidence against the band models is provided by paramagnetic neutron scattering experiments. These experiments confirm that the band splitting persists well above T_c and reveal that the paramagnetic response in pure γ-Fe [11], Fe_3Pt [12] and $Fe_{65}Ni_{35}$ [13] is ferromagnetically correlated. There is no evidence for the presence of antiferromagnetic correlations which are predicted, in some models, to characterize the low-moment state. The spatial distribution of the magnetic moment in a ferromagnet can be determined from precise measurements of the magnetic neutron scattering in the Bragg reflections. Such measurements can therefore be used to provide evidence for or against particular models of the invar effect. In the present paper we describe a series of experiments to determine the temperature dependence of the magnetization distribution in $Fe_{65}Ni_{35}$. The magnetic scattering amplitudes were obtained from the polarization dependence of the intensity of Bragg reflections. Measurements have been made at temperatures chosen to cover the region of anomalous thermal expansion and the paramagnetic regime where the thermal expansion has regained its normal Grüneisen behaviour.

2. Material

Using starting elements of 4N purity a crystal of $Fe_{65}Ni_{35}$ was grown using the Bridgman technique. Neutron Laue photographs confirmed that a 12 mm cube cut from the boule was a single crystal. Two smaller pieces suitable for polarized neutron diffraction were spark eroded from one edge of this crystal in the form of irregular pillars with dimensions of approximately $0.7 \times 0.7 \times 10\ \text{mm}^3$ and $2.2 \times 2.2 \times 5\ \text{mm}^3$. They both had a $[1\bar{1}0]$ direction parallel to the long axis. The smaller crystal allowed the strong low-angle reflections to be measured with only moderate extinction, while the larger crystal enabled good statistical accuracy to be obtained for the higher-angle reflections in which the magnetic scattering is very weak.

3. Polarized neutron diffraction measurements

Measurements of the polarization dependence of the peak intensity scattered by Bragg reflections (flipping ratio measurements) were made on the polarized neutron diffractometer D3 which receives neutrons from the ILL hot source. In order to determine the degree of extinction in the crystals measurements were made on both crystals in a field of 4.6 T at 100 K and with neutron wavelengths of 0.84, 0.71, 0.61 and 0.48 Å. With no correction for extinction the magnetic amplitude obtained for the strong 111 reflection from the larger crystal varied from 3.34(6) μ_B at 0.84 Å to 4.21(3) μ_B at 0.48 Å. The two parameters (domain radius and mosaic spread) of the Becker–Coppens extinction model [14] were determined from the wavelength and path-length dependence of the flipping ratios, using a procedure which minimized the spread in the magnetic scattering amplitudes obtained from all measurements of each independent reflection. It was found that the minimum spread for the six strongest reflections was obtained with a mosaic spread parameter of 3×10^{-4} radians^{-1} and a domain ratio of 1 μm.

The measurements as a function of temperature were made without the hot source present and were confined to a single wavelength 0.84 Å. The samples were magnetized using a vertical field of 9 T. A set of 62 reflections with $\sin\theta/\lambda \leqslant 1.0$ Å $^{-1}$ which were accessible within the geometric constraints of the instrument was established. This full set of reflections was measured for both crystals at 600, 500, 400 and 300 K, the highest temperature being above the Curie temperature (530 K). Measurements were also made on the larger crystal at 200 K and 100 K.

The magnetic structure amplitudes were calculated from the measured flipping ratios using the extinction parameters obtained at 100 K and taking into account the different sizes of the two crystals. The structure amplitudes of equivalent reflections were averaged and the standard deviations estimated from the differences of individual measurements from the mean.

4. Results

A simple atomic model has been used to describe the magnetic scattering. It consists of a random distribution of iron and nickel atoms on a fcc lattice in the proportion 65% iron to 35% nickel. The spherical component of the magnetization distribution around each atom corresponds to that of the d-electrons in a free atom of the appropriate species. An overall departure from spherical symmetry appropriate to the cubic crystal field is included by allowing the fraction of the d-electrons with e_g symmetry to vary. Using this model the structure factor $F(\boldsymbol{k})$ can be written

$$F(\boldsymbol{k}) = 4\left(\mu_O \langle j_0(\boldsymbol{k})\rangle_{Fe} + \mu_D\left(\langle j_0(\boldsymbol{k})\rangle_{Ni} - \langle j_0(\boldsymbol{k})\rangle_{Fe}\right) + \mu_A A(\boldsymbol{k})\langle j_4(\boldsymbol{k})\rangle_{Fe}\right). \tag{1}$$

In equation (1), $\langle j_0(\boldsymbol{k})\rangle_{Fe}$ and $\langle j_0(\boldsymbol{k})\rangle_{Ni}$ are the spherical parts of the iron and nickel form factors respectively. The first term is the dominant one; it is proportional to the total moment μ_O, and to that part of the magnetization, averaged over all sites, which has the same radial distribution as Fe 3d-electrons. The second term allows for some flexibility in the radial distribution. If the simple model described above is appropriate, then the average moment on each iron atom is $(\mu_O - \mu_D)/0.65$ and that on each nickel atom $\mu_D/0.35$. The equation is written in this way because there is rather little difference between the form factors $\langle j_0(\boldsymbol{k})\rangle_{Fe}$ and $\langle j_0(\boldsymbol{k})\rangle_{Ni}$ so that although the total moment μ_O is well determined, the values of the individual iron and nickel moments are highly correlated with one another. The asphericity of the moment distribution is described by the final term in equation (1).

$$A(\boldsymbol{k}) = \sqrt{\frac{5}{14}}\left(Y_4^4(\hat{\boldsymbol{k}}) + Y_4^{-4}(\hat{\boldsymbol{k}})\right) + Y_4^0(\hat{\boldsymbol{k}})$$
$$= \frac{h^4 + k^4 + l^4 - 3h^2k^2 - 3k^2l^2 - 3l^2h^2}{(h^2 + k^2 + l^2)^2}. \tag{2}$$

The fraction of electrons in orbitals of e_g symmetry is

$$\gamma = \frac{1}{5}\left(\frac{6\mu_A}{\mu_O} + 2\right). \tag{3}$$

Equation (1) was fitted to the experimental results by a least-squares procedure to give the parameters μ_O, μ_D and μ_A at each measurement temperature. The results of these fits are given in table 1 and as an example of the quality of agreement obtained, the observed and calculated values at 400 K are shown in figure 1. From table 1 it may be seen that below T_c a substantial moment resides on both the Fe and Ni sites and that in the paramagnetic phase

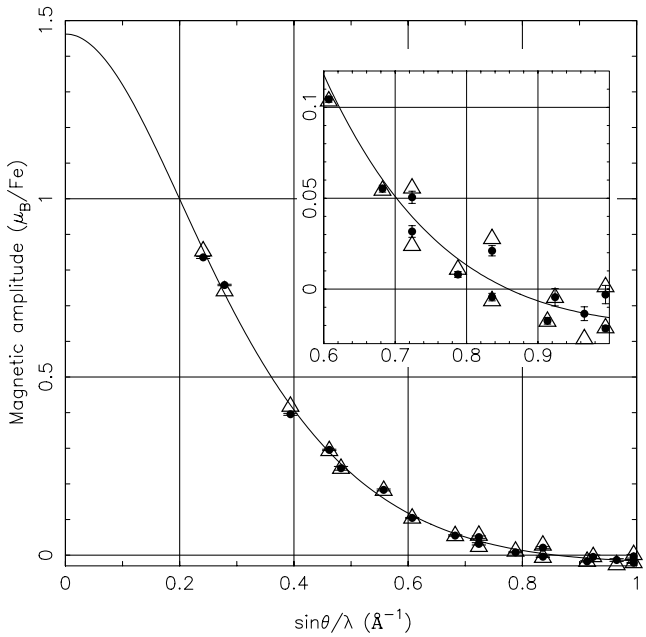

Figure 1. Observed and calculated values of the magnetic scattering per atom in $Fe_{65}Ni_{35}$ at 400 K in 9 T. The observed values are shown as full circles (●) with error bars, and the calculated values as open triangles (△). The inset shows the points with $\sin\theta/\lambda > 0.6$ Å^{-1} on a larger scale.

a significant moment is induced by 9 T. It is noteworthy that there is no significant change in the fraction of unpaired electrons with e_g symmetry between 100 K and 600 K. Any change in the shape of the radial part of the form factor will lead to variation in the ratio μ_D/μ_O which is shown in the final column of table 1. It can be seen that this parameter is also essentially constant between 100 K and 600 K.

Table 1. Results of least squares fit of the parameters of equation (1) to the magnetic structure factors of $Fe_{65}Ni_{35}$ measured in the temperature range 100–600 K.

T(K)	H(T)	$\mu_O(\mu_B)$	$\mu_D(\mu_B)$	$\mu_A(\mu_B)$	γ(%)	μ_D/μ_O
600	9.0	0.56(1)	0.12(3)	0.03(1)	47(2)	0.21(5)
500	9.0	0.98(2)	0.34(11)	0.08(2)	49(3)	0.35(12)
400	9.0	1.46(2)	0.29(8)	0.09(2)	47(2)	0.20(5)
300	9.0	1.79(3)	0.48(10)	0.13(3)	48(2)	0.27(6)
200	9.0	2.10(5)	0.52(9)	0.11(1)	46.3(1.2)	0.25(4)
100	9.0	2.3(1)	0.44(11)	0.14(2)	47.5(1.5)	0.19(5)
100	4.6	1.90(3)	0.39(5)	0.08(1)	45.9(4)	0.21(3)

5. Discussion

The magnetic form factor determined in the present study is in reasonable agreement with the results of earlier investigations undertaken at 77 and 300 K [18]. The new results extend to slightly higher values of $\sin\theta/\lambda$ and should therefore give a more precise value of γ. These measurements can be interpreted simply, only if magnetic moments exist on both the iron and nickel atoms. This is in contradiction with certain band models which give zero moment on the nickel atoms. The absence of any change in the form factor as a function of temperature places further severe constraints on band models which can be used to account for the invar effect.

It is interesting to trace the evolution of the percentage occupancy of the e_g orbitals in Fe–Ni alloys as a function of composition. The data available are given in table 2 and include values for alloys containing 28 and 50 atomic % Fe which were measured in the present series of experiments. The table shows that the e_g population rises steadily to about 47% at the invar composition where it is independent of temperature between 100 K and 600 K. This value is rather close to that for α iron (53%) where, in the bcc structure, the e_g lobes point towards nearest neighbours. It suggests that this high e_g population is a precursor of the fcc–bcc martensitic transformation. It may be significant that essentially the same value of γ has been measured recently for the ordered Fe_3Pt invar compound [19] which is also on the verge of a martensitic transformation.

Electronic structure and total energy calculations for fcc iron predict the existence of more than one magnetic state providing support for the basic premise of the two-state model. The number, nature and volume dependence of these states depends on the approximations used in the calculations. However, the thermal repopulation of the low-, at the expense of the high-, spin states is still invoked as the underlying reason for the invar effect. Details of the various band models have been discussed by Entel [6] who also investigated the connection between the martensitic transformation, the invar effect and the magneto volume instabilities brought about by the low-moment–high-moment transitions. The calculations which were carried out for Fe_3Ni provided specific information on the volume dependence of the electron occupation and magnetization of e_g and t_{2g} orbitals. At a critical volume the calculations indicated that the system could exist in either the low- or high-moment state with different

Table 2. The percentage γ of electrons in orbitals of e_g symmetry in some disordered $Fe_xNi_{(1-x)}$ alloys.

x	Structure	T(K)	γ(%)	Ref.
0	fcc	300	19	[20]
0.25	fcc	300	37.5(17)	[21]
0.28	fcc	300	37.6(3)	This work
0.50	fcc	300	45.6(12)	[21]
0.50	fcc	100	45.0(5)	This work
0.505	fcc	300	49(3)	[22]
0.65	fcc	100	46(1)	This work
0.65	fcc	300	48(2)	This work
0.66	fcc	77	47.9	[18]
0.66	fcc	300	44.6	[18]
1.00	bcc	300	53	[23]

wave functions and correspondingly different spin and charge densities but with essentially the same energy. The invar behaviour is characterized by an anomalously large transfer of charge from e_g to t_{2g} orbitals. On the low-spin side the moments are predicted to be mostly of t_{2g} character whilst on the high-spin side they are mostly of e_g character. However, the polarized neutron measurements, which cover the range in temperature over which thermal repopulation is predicted to take place, show that there is no change in the ratio of the e_g to t_{2g} carriers indicating no change in the symmetry of the time averaged moment.

It may be concluded that the interpretation of the invar effect based on the static interpretation of band structure calculations is incorrect. However, although the present experiment shows that the time averaged magnetization distribution does not change with temperature, it is not sensitive to correlations between the electronic configuration and the lattice vibrations. Recent neutron inelastic scattering studies on $Fe_{65}Ni_{35}$ have demonstrated that such correlations do indeed exist [24]. These, together with the present results, suggest that further progress in understanding the invar effect may be obtained by considering the dynamic implications of instabilities in the band structure.

Acknowledgments

We would like to thank E Lelievre, E Bourgeat Lami and S Pujol for their work in developing the high temperature insert, for the 10 T superconducting magnet, without which this experiment would not have been possible.

References

[1] Guillaume Ch E 1897 *C.R. Acad. Sci.* **10** 235
[2] Schilfgarde M V, Abrikosov I A and Johanson B 1999 *Nature* **400** 46
[3] Mohn P 1999 *Nature* **400** 18
[4] Lynn J W, Rosov N, Acet M and Bach H 1994 *J. Appl. Phys.* **75** 6069
[5] Weiss R J 1963 *Proc. Roy. Soc.* **82** 281
[6] Entel P, Hoffmann E, Mohn P, Schwarz K and Moruzzi V L 1993 *Phys. Rev.* B **47** 8706
[7] Matsui M, Adachi K and Chikazumi S 1980 *J. Appl. Phys.* **51** 6319
[8] Hasegawa H 1981 *J. Phys. C: Solid State Phys.* **14** 2793
[9] Wassermann E F 1990 *Ferromagnetic Materials* ed K H J Buschow and E P Wohlfarth (Amsterdam: Elsevier) vol 5 p 238
[10] Yamada O 1983 *Physica B* **119** 90

[11] Brown P J, Capellmann H, Deportes J, Givord D and Ziebeck K R A 1983 *J. Magn. Magn. Mater.* **31–34** 295
[12] Ziebeck K R A, Webster P J, Brown P J and Capellmann H 1983 *J. Magn. Magn. Mater.* **36** 151
[13] Tajima K, Boïi P, Shirane G, Ishikawa Y and Kohgi M 1987 *Phys. Rev.* B **35** 274
[14] Becker P J and Coppens P 1974 *Acta Cryst.* A **30** 139
[15] Yamada O, Ono F and Nakai I 1977 *Physica* B **91** 298
[16] Chikazumi S 1979 *J. Magn. Mag. Mater.* **10** 113
[17] Shiga M 1967 *J. Phys. Soc. Japan* **22** 539
[18] Ito Y, Akimitsu J, Matsui M and Chikazumi S 1979 *J. Magn. Magn. Mater.* **10** 194
[19] Brown P J, Chatterji T, Kaestner J, Neumann K-U, Wassermann W F and Ziebeck K R A 2000 unpublished
[20] Mook H A and Shull C G 1966 *J. Appl. Phys.* **37** 1034
[21] Cable J W and Wollan E O 1973 *Phys. Rev.* B **7** 2005
[22] Menzinger F, Sachetti F and Leone F 1974 *Il Nuovo Cimento* **20 B** 1
[23] Shull C G and Yamada Y 1962 *J. Phys. Soc. Japan Suppl.* **B-III** 1
[24] Brown P J, Roessli B, Smith J G, Neumann K-U and Ziebeck K R A 1996 *J. Phys.: Condens. Matter* **8** 1527